collisions are shielded by both electrons and ions. However, in electron-electron collisions, $(E_1'-E_1)/q$ is of the order of the typical electron velocity; since this is much greater than the mean ion velocity, ions are completely ineffective in shielding ee collisions.

[8]S. Chapman and T. G. Cowling, The Mathematical Theory of Non-Uniform Gases (Cambridge University Press, Cambridge, England, 1961).

[9]These definitions follow those of Chapman-Cowling, Chap. 8. The subsequent calculation is also closely analogous to that of Chapman-Cowling in the nondegenerate case. Transport coefficients are often defined in the following alternative way:

$$J = eS_{11}[e\vec{E} + T\nabla(\mu/T)] + eS_{12}\nabla T/T,$$

$$Q = -S_{21}[e\vec{E} + T\nabla(\mu/T)] - S_{22}\nabla T/T.$$

The S_{ij} are related to the S_{ij}' by $S_{11} = S_{11}'$; $S_{12} = S_{12}' + \frac{5}{3}\mathcal{E}S_{11}'$; $S_{22} = S_{22}' + (10/3)\mathcal{E}S_{12}' + (5\mathcal{E}/3)^2 S_{11}$.

[10]In Ref. 3, the degenerate plasma is studied in detail for all values of D_e/λ. It is shown that, in a deep sense, the real transition from nondegenerate to highly degenerate behavior occurs not in the region $\alpha \sim 1$, but rather for $\alpha \gg 1$, $D_e/\lambda \sim 1$. This is true because, in our weakly coupled system, the ratio of momentum transfer in a typical collision to thermal width of the Fermi surface is λ/D_e, rather than α as in system with strong interactions. The transition studied in the present paper, for $-1 \lesssim \alpha \lesssim 1$, is relatively superficial (which is why the mathematics can be done so simply). A plasma obeys the Fermi liquid theory of Abrikosov and Khalatnikov, Rept. Progr. Phys. 22, 329 (1959), only if $D_e/\lambda \ll 1$.

[11]This simple procedure gives the coefficient of the logarithm exactly, but gives the argument of the logarithm correct to within a factor of order unity. Thus the ee collision contribution to the transport coefficients is accurate to within order $1/\ln(D_e/\lambda)$, and the ei contribution (discussed later) to within order $1/\ln(D/\lambda')$. There is little point in calculating the argument of the logarithm more accurately, since the effects of dynamic shielding, which have been neglected, also are of this order. In Refs. 2 and 3, dynamic shielding is included for the cases of nondegenerate and highly degenerate electrons, respectively, and the corrections of order $1/\ln(D_e/\lambda)$ and $1/\ln(D/\lambda')$ are found.

[12]W. B. Hubbard, Astrophys. J. 146, 856 (1966).

[13]W. B. Hubbard and M. Lampe, to be published.

PHYSICAL REVIEW VOLUME 174, NUMBER 1 5 OCTOBER 1968

Asymptotic Behavior of the Pair Distribution Function of a Classical Electron Gas

D. J. Mitchell and B. W. Ninham

Department of Applied Mathematics, University of New South Wales, Kensington, New South Wales, Australia

(Received 6 May 1968)

The asymptotic behavior of the pair distribution function of a classical electron gas is determined. The result is in disagreement with the form conjectured by Lie and Ichikawa.

1. INTRODUCTION

During recent years[1] the pair distribution function (PDF) of the classical electron gas has been extensively investigated by many authors using either the Mayer cluster-expansion method or the Bogoliubov-Born-Green-Kirkwood-Yvon (BBGKY) hierarchy equations. The PDF has been evaluated by diagram techniques by Bowers and Salpeter,[2] De Witt,[3] and others to order ϵ^2, where $\epsilon = (4\pi\beta^3\rho e^6)^{1/2}$ is the dimensionless plasma parameter, while Lie and Ichikawa[4] have reviewed the work of many authors who approached the problem via the kinetic equations. The result for the radial distribution function given by Bowers and Salpeter (BS) is

$$g^{\mathrm{BS}}(r) = \exp(-\epsilon x^{-1}e^{-x}) + W_1(x), \tag{1.1}$$

where $$W_1(x) = -\tfrac{1}{8}\epsilon^2 x^{-1}[\tfrac{4}{3}(e^{-x} - e^{-2x}) + (3-x)[\ln 3 - E_1(x)]e^{-x} + (3+x)E_1(3x)e^{x}], \tag{1.2}$$

with $$x = r/\Lambda_D, \quad \Lambda_D = (4\pi\beta\rho e^2)^{-1/2}, \quad E_1(x) = \int_x^\infty (e^{-y}/y)dy. \tag{1.3}$$

In Eq. (1.1), $g(r)$ is defined by the relation

$$\rho^2 g(r) = n_2(\vec{r}_1, \vec{r}_2) = n_2(|\vec{r}_1 - \vec{r}_2|) = n_2(r), \tag{1.4}$$

where $n_2(r)$ is the PDF. At large distances, Eq. (1.1) has the asymptotic form

$$g(r) \sim 1 - \epsilon x^{-1}e^{-x} + \tfrac{1}{8}\epsilon^2 \ln 3\, e^{-x} + O(e^{-2x}). \tag{1.5}$$

De Witt[3] observed that the second term of Eq. (1.5) dominates the Debye-Huckel term as $x \to \infty$, and related this to a similar phenomenon which occurs in the study of the dynamic behavior of a plasma. Such a conclusion is physically unreasonable, and Lie and Ichikawa[4] have shown that the expansion Eq. (1.5) in powers of ϵ breaks down at very large distances $x > 8/\epsilon \ln 3$. These authors conjectured further that the correct behavior of $g(r)$ is

$$g(r) \sim 1 - \epsilon x^{-1} \exp[-x - \psi(x)] , \tag{1.6}$$

where $$\psi(x) \sim \tfrac{1}{8}\epsilon \ln 3 \exp[-\tfrac{1}{8}\epsilon x \ln 3] \tag{1.7}$$

is a function which tends to zero as $x \to \infty$.

We shall show, by the Mayer cluster-expansion method, that this conjecture is incorrect, and that the correct asymptotic form of $g(r)$ is

$$g(r) \sim 1 - (A/x) e^{-Bx} , \tag{1.8}$$

where

$$A = \epsilon + (\tfrac{3}{8}\ln 3 + \tfrac{1}{6})\epsilon^2 + O(\epsilon^3 \ln \epsilon) , \quad B = 1 + \tfrac{1}{8}\epsilon \ln 3 + \tfrac{1}{12}\epsilon^2 \ln \epsilon + 0.066\epsilon^2 + O(\epsilon^3 \ln \epsilon) . \tag{1.9}$$

2. CLUSTER-INTEGRAL EXPANSION

2.1 Montroll-Mayer Expansion

To avoid any confusion with respect to terminology, we first summarize briefly the formulation of the problem as given by Montroll and Mayer.[5] In standard notation the classical PDF in the grand canonical ensemble is defined as

$$n_2(\vec{r}_1, \vec{r}_2) = Z_G^{-1} \sum_N z^N Z_N n_2^{(N)}(\vec{r}_1, \vec{r}_2) , \tag{2.1}$$

where $$n_2^{(N)}(r_1, r_2) = [(N-2)!\, Z_N]^{-1} (2\pi\hbar)^{-3N} \int d^{3N}p \int d^3 r_3 \cdots d^3 r_N \exp[-\beta E_N(p, r)] \tag{2.2}$$

is the PDF for an N-particle system, z is the fugacity, Z_N is the partition function, and Z_G the grand partition function. The energy for an N-particle system is

$$E_N(p, r) = \sum_j \frac{p_j^2}{2m} + \sum_{i<j} \phi(\vec{r}_i - \vec{r}_j) , \tag{2.3}$$

where $\phi(r)$ is the two-body potential. After carrying out the momentum integrations, Eq. (2.1) can be written in the form

$$n_2(\vec{r}_1, \vec{r}_2) = \frac{1}{Z_G} \sum_N z_0^N \frac{1}{(N-2)!} \int d^3 r_3 \cdots d^3 r_N \prod_{i<j} (1 + f_{ij}) , \tag{2.4}$$

where $$z_0 = [z/(2\pi\hbar)^3]\,(2\pi m/\beta)^{3/2} \tag{2.5}$$

and $$f_{ij} = \exp[-\beta\phi(\vec{r}_2 - \vec{r}_j)] - 1 . \tag{2.6}$$

If we expand the product in Eq. (2.4), we obtain an expression for $n_2(\vec{r}_1, \vec{r}_2)$ as an infinite sum of terms which can be put into a one to one correspondence with a set of labeled diagrams. These diagrams contain two or more vertices (labeled $1, 2, 3, \ldots$) with at most one line (f bond) between each pair of vertices. Each bond corresponds to a factor f_{ij} in the corresponding term. For example, the term

$$(z_0^4/2!\, Z_G) \int d^3 r_3\, d^3 r_4 f_{13} f_{14} f_{34} f_{23} f_{24} \tag{2.7}$$

is represented by the diagram Fig. 1(a) Diagrams may be connected or disconnected. A diagram is disconnected if it contains two groups such that no vertex of one group is connected by an f bond to any vertex of another group. Thus Fig. 1(b) is disconnected, whereas Fig. 1(a) is connected.

We shall call the factor $\int d^3 r_3 \cdots d^3 r_N$ (product of f_{ij}'s) the integral associated with the diagram, and the remaining factor the weight factor for the diagram. By a lengthy but straightforward argument it can be shown (see, e.g., Salpeter,[5] and, for the quantum-mechanical case, Montroll[6]) that

$$n_2(\vec{r}_1, \vec{r}_2) = \rho^2 + \sum_{k=2}^{\infty} b_k(\vec{r}_1, \vec{r}_2) z_0^k , \tag{2.8}$$

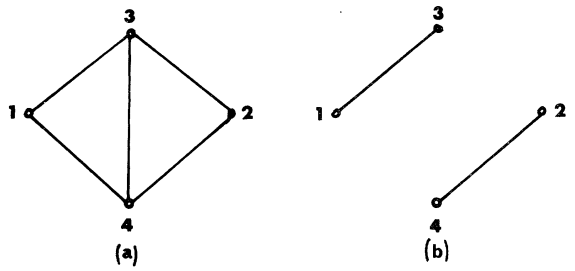

FIG. 1. (a) Connected and (b) disconnected diagrams.

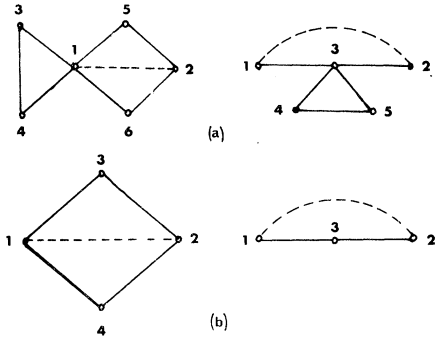

FIG. 2. (a) Reducible and (b) irreducible diagrams.

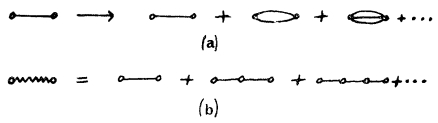

FIG. 3. (a) ϕ bonds and (b) screened ϕ bonds.

where

$$b_k(\vec{r}_1,\vec{r}_2)=[(k-2)!]^{-1}\text{(sum of integrals associated with all connected labeled diagrams containing } k \text{ vertices including } \langle 1\rangle \text{ and } \langle 2\rangle). \tag{2.9}$$

The expression Eq. (2.8) is inconvenient insofar as it contains the fugacity. A further simplification can be effected if the remaining diagrams are classified into two classes, reducible and irreducible. A diagram is reducible if after joining $\langle 1\rangle$ and $\langle 2\rangle$ by an extra bond and erasing one vertex it becomes disconnected. Examples of reducible and irreducible diagrams are given in Figs.2(a) and 2(b). By a lengthy combinatorial argument it can then be shown (see, e.g., Salpeter[5]) that

$$n_2(\vec{r}_1,\vec{r}_2)=\rho^2+\sum_{k=2}^{\infty}\beta_k(\vec{r}_1,\vec{r}_2)\rho^k\,, \tag{2.10}$$

where

$$\beta_k(\vec{r}_1,\vec{r}_2)=[(k-2)!]^{-1}\text{ (sum of integrals corresponding to all connected, labeled irreducible diagrams containing } k \text{ vertices including } \langle 1\rangle \text{ and } \langle 2\rangle). \tag{2.11}$$

This result was first derived by Mayer and Montroll.[7]

In the thermodynamic limit $n_2(\vec{r}_1,\vec{r}_2)$ is a function of $r=|\vec{r}_1-\vec{r}_2|$ only, and the radial distribution function $g(r)$ in terms of diagrams becomes

$$g(r)=1+\sum_{k=2}^{\infty}\beta_k(\vec{r}_1,\vec{r}_2)\rho^{k-2}\,. \tag{2.12}$$

2.2 ϕ Bonds.

To overcome divergence difficulties, it is usually convenient when dealing with the Coulomb gas to expand each factor f_{ij} which appears in a diagram as a power series in ϕ. From Eq. (2.6), we have

$$f_{ij}=\sum_{m=1}^{\infty}\frac{(-\beta)^m}{m!}(\phi_{ij})^m\,. \tag{2.13}$$

In terms of diagrams a single f bond can be represented as a sum of ϕ bonds as in Fig. 3(a). We can then express $g(r)-1$ in a slightly different form as the sum of connected labeled irreducible diagrams with ϕ bonds. These new diagrams may have any number of bonds between each pair of vertices. The contribution of a diagram with k vertices and l ϕ-bonds is

$$[(k-2)!\prod_{i<j}(m_{ij})!]^{-1}\rho^{k-2}(-\beta)^l\int d^3r_3\cdots d^3r_k\,(\text{product of } \phi_{ij}\text{'s, one } \phi_{ij} \text{ corresponding to each } \phi \text{ bond}). \tag{2.14}$$

It is clear that diagrams which can be derived from each other by permutation of vertices (not including $\langle 1\rangle$ or $\langle 2\rangle$ which are special) give equal contributions to $g(r)$. Therefore it is customary to introduce the notion of an unlabeled diagram. An unlabeled diagram (in which only the vertices $\langle 1\rangle$ and $\langle 2\rangle$ are labeled) is equal to the sum of the corresponding labeled diagrams which differ from each other only in a permutation of the vertices. An unlabeled diagram then carries an additional weighting factor equal to the number of labeled diagrams it contains.

Divergence difficulties associated with the long-range nature of the Coulomb interaction can now be removed if we perform a partial sum over chains of ϕ bonds. The new (screened) interaction which we represent by a wavy line, is represented diagrammatically in Fig.3(b). Just as a single ϕ bond represents $\phi(r)$, a wavy line represents a screened potential $\phi_s(r)$ given by the equations

$$\phi_s(r) = \int d^3\omega\, e^{i\vec{\omega}\cdot\vec{r}}\, \nu_s(\omega)\,, \tag{2.15}$$

$$\nu_s(\omega) = \nu(\omega)/[1 + 8\pi^3\rho\nu(\omega)]\,, \tag{2.16}$$

$$\nu(\omega) = (2\pi)^{-3}\int e^{-i\vec{\omega}\cdot\vec{r}}\,\phi(r)d^3r\,. \tag{2.17}$$

For the electron gas we have

$$\phi(r) = e^2/r,\quad \phi_s(r) = (e^2/r)e^{-\kappa_0 r},\quad \nu_s(\omega) = e^2/2\pi^2(\omega^2+\kappa_0^2)\,, \tag{2.18}$$

where $\kappa_0 = (4\pi\beta\rho e^2)^{1/2}$ is the inverse of the Debye screening length Λ_D.

3. THE ELECTRON GAS

3.1 Known Results

The diagrams of Fig. 4 were evaluated by Bowers and Salpeter,[2] De Witt,[3] and other authors. Diagrams Fig.4(a), 1, 2, 3... give contributions of

$$-\epsilon x^{-1}e^{-x}, (2!)^{-1}(-\epsilon x^{-1}e^{-x})^2, (3!)^{-1}(-\epsilon x^{-1}e^{-x})^3, \ldots, \tag{3.1}$$

whose sum is simply

$$g_a(r) = \exp(-\epsilon x^{-1}e^{-x}) - 1\,. \tag{3.2}$$

The diagrams of Fig.4(b) give a contribution $g_b(r)$, where

$$g_b(r) = (-2)(\beta^3\rho/2!)\int d^3r_3\phi_s^2(r_{13})\phi_s(r_{23}) = -\tfrac{1}{2}\epsilon^2 x^{-1}[e^{-x}\ln 3 - e^{-x}E_1(x) + e^{x}E_1(3x)]\,. \tag{3.3}$$

Finally, the diagram Fig.3(c) gives

$$g_c(r) = (\beta^4\rho^2/2!)\int d^3r_3 d^3r_4\phi_s(r_{13})\phi_s^2(r_{34})\phi_s(r_{42}) = \tfrac{1}{8}\epsilon^2 x^{-1}[(1+x)e^{-x}\ln 3 - \tfrac{4}{3}(e^{-x}-e^{-2x}) - (1+x)e^{-x}E_1(x) + (1-x)E_1(3x)]\,. \tag{3.4}$$

Summing Eqs. (3.2), (3.3), and (3.4), we obtain the Bowers-Salpeter expression for the radial distribution function already quoted above in Eqs. (1.1) and (1.2). All diagrams which remain are of higher order in ϵ. Using the well-known relation between the correlation energy per particle E and $g(r)$, viz.,

$$E = \tfrac{1}{2}\rho\int d^3r\,\phi(r)[g(r)-1] \tag{3.5}$$

we can obtain from Eqs. (1.1) and (1.2) the Abe[4] result for the correlation energy, which is

$$E/kT = -\tfrac{1}{2}\epsilon - \tfrac{1}{4}\epsilon^2\ln\epsilon - \tfrac{1}{2}(\gamma - \tfrac{2}{3} + \tfrac{1}{2}\ln 3)\epsilon^2\,, \tag{3.6}$$

where γ is Euler's constant. For large distances ($x \gg 1$), as already noted, the Bowers-Salpeter expression for the radial distribution function has the asymptotic form

$$g(r) \sim 1 - \epsilon x^{-1}e^{-x} - \epsilon^2(\tfrac{1}{6} + \tfrac{3}{8}\ln 3)x^{-1}e^{-x} + \tfrac{1}{8}\epsilon^2\ln 3 e^{-x} + O(e^{-2x})\,. \tag{3.7}$$

The term $\frac{1}{8}\epsilon^2\ln 3 e^{-x}$ dominates the Debye-Huckel term $-\epsilon x^{-1}e^{-x}$ for sufficiently large distances, an unacceptable result. However, this difficulty can be overcome by summing a wider class of diagrams.

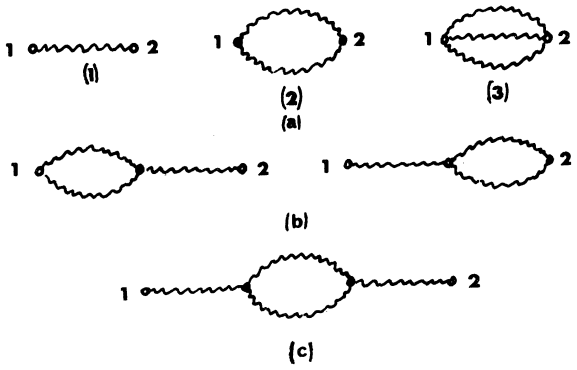

FIG. 4. Low-order diagrams.

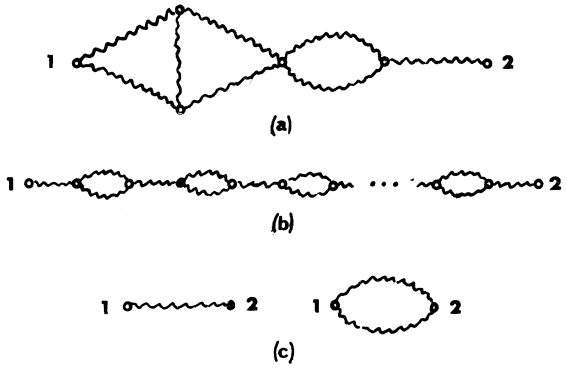

FIG. 5. Chains and mixed chains.

3.2 Mixed Chains

The evaluation of diagrams which may be regarded as chains linked together by single vertices, e.g., the diagram of Fig. 5(a), may be simplified through the following observation. Consider n diagrams linked together in a chain in such a way that each adjacent pair of diagrams shares only one vertex. Let the contributions of the individual component diagrams be $D_1(\vec{r}_1-\vec{r}_2)$, $D_2(\vec{r}_1-\vec{r}_2),\ldots,$ $D_n(\vec{r}_1-\vec{r}_2)$. Then the contribution of the whole chain is clearly

$$I=\rho^{n-1}\int d^3r_3\cdots d^3r_{n+1}D_1(\vec{r}_1-\vec{r}_3)D_2(\vec{r}_3-\vec{r}_4)\cdots D_n(\vec{r}_{n+1}-\vec{r}_2)\,. \tag{3.8}$$

In terms of Fourier transforms defined by

$$\bar{D}_k(\omega)=(2\pi)^{-3}\int d^3r\,e^{-i\vec{\omega}\cdot\vec{r}}D_k(r);\quad D_k(r)=\int d^3\omega\,e^{i\vec{\omega}\cdot\vec{r}}\bar{D}_k(\omega)\,, \tag{3.9}$$

Eq. (3.8) becomes

$$I=\rho^{n-1}\int d^3r_3\cdots d^3r_{n+1}\int d^3\omega_1\cdots d^3\omega_n e^{i\vec{\omega}_1\cdot(\vec{r}_1-\vec{r}_3)}e^{i\vec{\omega}_2\cdot(\vec{r}_3-\vec{r}_4)}\cdots e^{i\vec{\omega}\cdot(\vec{r}_{n+1}-\vec{r}_2)}[\bar{D}_1(\omega_1)\cdots\bar{D}_2(\omega_n)]$$
$$=[(2\pi)^3\rho]^{n-1}\int d^3\omega\,\bar{D}_1(\omega)\cdots\bar{D}_n(\omega)e^{i\vec{\omega}\cdot(\vec{r}_1-\vec{r}_2)}\,. \tag{3.10}$$

Consider the mixed chain shown in Fig. 5(b). The component diagrams are shown in Fig. 5(c). The first of these components gives a contribution

$$D_1(r)=-\epsilon x^{-1}e^{-x},\quad \bar{D}_1(\omega)=-(\epsilon/2\pi^2\kappa_0 3)(\Omega^2+1)^{-1} \tag{3.11}$$

while for the second we have

$$D_2(r)=\tfrac{1}{2}(-\epsilon x^{-1}e^{-x})^2,\quad \bar{D}_2(\omega)=(\epsilon^2/4\pi^2\kappa_0^3)\,\Omega^{-1}\tan^{-1}(\Omega/2)\,. \tag{3.12}$$

In Eqs. (3.11) and (3.12) we have written $\omega=\kappa_0\Omega$ for notational convenience. Let $n+1$ and n be the number of times the components 1 and 2 occur in the mixed chain. Its contribution is then, by Eq. (3.10),

$$[(2\pi)^3\rho/\kappa_0^3]^{2n}\int d^3\Omega[-\epsilon/2\pi^2(\Omega^2+1)]^{n+1}[(\epsilon^2/4\pi^2\Omega)\tan^{-1}(\Omega/2)]^n e^{i\vec{\Omega}\cdot\vec{x}}=-(\epsilon/2\pi^2)(-\epsilon/2)^n\int d^3\Omega\,e^{i\vec{\Omega}\cdot\vec{x}}$$
$$\times[\tan^{-1}(\Omega/2)]^{-n}/\Omega^n(\Omega^2+1)^{n+1}=-(\epsilon/\pi ix)(-\epsilon/2)^n\int_{-\infty}^{\infty}e^{i\Omega x}[\tan^{-1}(\Omega/2)]^n/\Omega^{n-1}(\Omega^2+1)^{n+1}d\Omega\,. \tag{3.13}$$

The dominant term in the integral of Eq. (3.13) for large x is $2\pi i$ times the residue at the pole at $\Omega=i$. This is a polynomial in x of degree n times e^{-x}/x. The sum of these mixed chains therefore gives a power series in x multiplied by e^{-x}/x. The expression Eq. (3.7) includes only the first two terms of this power series. The Bowers-Salpeter result for $g(r)$ is then a useful expression for computational purposes only in the intermediate distance region $x<8/\epsilon\ln 3$.

Summing Eq. (3.13) over n, $n=0,1,2,\ldots$, we have for the sum of all mixed chains the expression

$$g_{\mathrm{mc}}(r)=-(\epsilon/\pi ix)\int_{-\infty}^{\infty}\Omega e^{i\Omega x}d\Omega/[\Omega^2+1+(\epsilon/2\Omega)\tan^{-1}(\Omega/2)]\,. \tag{3.14}$$

It is easily shown that Eq. (3.14) has a simple pole at $\Omega=iB$, where B is real and $1<B<3/2$, and $B\approx 1$. The asymptotic form of Eq. (3.14) is then

$$g_{mc}(r) \sim -Ax^{-1}e^{-Bx}, \tag{3.15}$$

where $A \simeq \epsilon$, $B \simeq 1$. This result was apparently known to Hirt.[8]

4. ELIMINATION OF CHAINS

4.1 General Formulas

A partial sum of diagrams which includes the mixed chains then shows explicitly that the Bowers-Salpeter and Lie and Ichikawa expressions are the leading terms of a power series in ϵ useful for computation only for distances $x < 8/\epsilon \ln 3$. However, to establish the correct form of the PDF at large distances it is necessary to effect a further simplification. We consider all unlabeled connected irreducible diagrams with (unscreened) ϕ bonds. These diagrams may be divided into two classes: chains which consist of diagrams linked together as in Sec. 3.2 above, and the remaining diagrams which we call simple diagrams. Let $g^*(r)$ be the sum of all simple diagrams. Then Eq. (3.10) which expresses a chain in terms of the simple diagrams from which it is formed, gives

$$g(r) = 1 + \kappa_0^3 \sum_{n=1}^{\infty} [(2\pi)^3\rho]^{n-1} \int d^3\Omega [\bar{g}^*(\Omega)]^n e^{i\vec{\Omega}\cdot\vec{x}} = 1 + \kappa_0^3 \int d^3\Omega \frac{\bar{g}^*(\Omega)\, e^{i\vec{\Omega}\cdot\vec{x}}}{[1 - (2\pi)^3\rho\bar{g}^*(\Omega)]}, \tag{4.1}$$

where $\bar{g}^*(\Omega) = (2\pi\kappa_0)^{-3} \int e^{-i\vec{\Omega}\cdot\vec{x}} g^*(r) d^3x$. (4.2)

The expression Eq. (4.1) can be recast into a more convenient form as follows. Let $g_0(r)$ be the sum of all simple diagrams except the simplest, viz., 1⟷2. Then

$$\bar{g}_0(\Omega) = \bar{g}^*(\Omega) - (\epsilon/2\pi^2\kappa_0^3)\Omega^{-2}, \tag{4.3}$$

so that Eq. (4.1) becomes

$$g(r) = 1 + \int d^3\Omega e^{i\vec{\Omega}\cdot\vec{x}} [\kappa_0^3\bar{g}_0(\Omega) - (\epsilon/2\pi^2\Omega^2)] \{1 - [(2\pi)^3\rho/\kappa_0^3][\kappa_0^3\bar{g}_0(\Omega) - (\epsilon/2\pi^2\Omega^2)]\}^{-1}$$

$$= 1 - \frac{\epsilon}{2\pi^2} \int d^3\Omega e^{i\vec{\Omega}\cdot\vec{x}} \frac{1 - 8\pi^3\rho\Omega^2\bar{g}_0(\Omega)}{\Omega^2 + 1 - 8\pi^3\rho\Omega^2\bar{g}_0(\Omega)} = 1 - \frac{\epsilon}{\pi i x} \int_{-\infty}^{\infty} \Omega d\Omega\, e^{i\Omega x} \frac{1 - 8\pi^3\rho\Omega^2\bar{g}_0(\Omega)}{\Omega^2 + 1 - 8\pi^3\rho\Omega^2\bar{g}_0(\Omega)}, \tag{4.4}$$

where we have carried out the angular integration and used the identity

$$2\pi^2\kappa_0^3/\epsilon = 8\pi^3\rho. \tag{4.5}$$

It can be shown that this result Eq. (4.4) holds also if the ϕ bonds are screened. We therefore consider simple diagrams to be constructed with screened ϕ bonds.

4.2 Explicit Evaluation of $\bar{g}_0(\Omega)$

In order to determine the explicit asymptotic form of $g(r)$ we now consider the diagrams which contribute to $\bar{g}_0(\Omega)$. Some of the low-order diagrams which contribute to $\bar{g}_0(\Omega)$ are shown in Fig. 6, and Figs. 6(a)–(f) exhaust all relevant diagrams up to and including order ϵ^3.

The lowest-order diagram Fig. 6(a) has a Fourier transform

$$\bar{g}_0(\Omega)[6a] = (\epsilon^2/4\pi^2\kappa_0^3\Omega)\tan^{-1}(\Omega/2). \tag{4.6}$$

This function has branch points at $\Omega = \pm 2i$, but is analytic in the plane shown in Fig. 7. All remaining simple diagrams are $O(\epsilon^3 \ln\epsilon)$. Hence if we approximate $\bar{g}_0(\Omega)$ by Eq. (4.6), substitute this result into Eq. (4.4), and close the contour as indicated in Fig. 7, we obtain

$$g(r) \sim 1 - Ax^{-1}e^{-Bx} + O(e^{-2x}), \tag{4.7}$$

where $A = \epsilon + O(\epsilon^2)$, $B = 1 + \frac{1}{8}\epsilon \ln 3 + \cdots$ (4.8)

and $(\kappa_0 B)^{-1}$ is a modified Debye screening length. Comparison with the asymptotic form suggested by Lie and Ichikawa, Eqs. (1.6) and (1.7), then shows that we cannot yet disprove this conjecture, which implies that for large distances, the Debye screening length is identically $\Lambda_D = (\kappa_0)^{-1}$. (Up to terms of order ϵ^2, the two results agree.) It is therefore necessary to consider higher-order diagrams.

Note that in position space, the diagram Fig. 6(a) has a contribution

$$g_0(r)[6a] = \tfrac{1}{2}\epsilon^2 x^{-2} e^{-2x} = O(e^{-2x}). \tag{4.9}$$

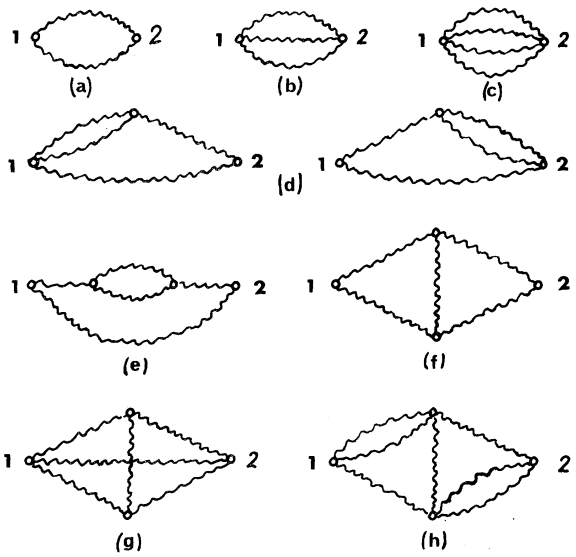

FIG. 6. Simple diagrams which contribute to $\bar{g}_0(\Omega)$.

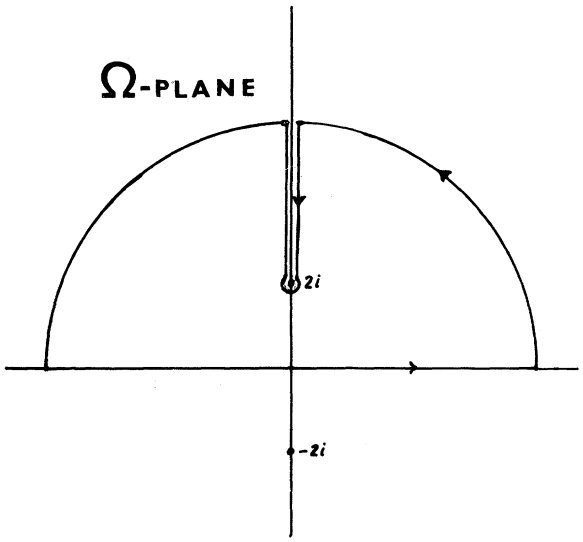

FIG. 7. Contour for evaluation of $g(r)$.

It seems likely, as we shall see below, that all diagrams which contribute to $g_0(r)$ are $O(e^{-2x})$. A corollary of this assumption, which we shall use, is that

$$\bar{g}_0(\Omega) = (2\pi\kappa_0)^{-3}\int d^3x\, e^{-i\vec{\Omega}\cdot\vec{x}} g_0(x) = (2\pi^2\kappa_0{}^3\Omega)^{-1}\int_0^\infty x\,\sin\Omega x\, g_0(x)dx \tag{4.10}$$

is analytic in the strip $|\mathrm{Im}\Omega|<2$.

The next diagram of the set which contributes to $g_0(\Omega)$ is shown in Fig.6(b). Its contribution is

$$g_0(r)[6b] = (3!)^{-1}(-\epsilon x^{-1}e^{-x})^3 , \tag{4.11}$$

The Fourier transform of this expression diverges. However, the sum of all ladders, of which Figs. 6(b) and 6(c) are typical is

$$g_0(r)[L] = \exp(-\epsilon x^{-1}e^{-x}) - 1 + \epsilon x^{-1}e^{-x} - (2!)^{-1}(\epsilon x^{-1}e^{-x})^2 \tag{4.12}$$

with Fourier transform

$$\bar{g}_0(\Omega)[L] = \frac{i}{(2\pi\kappa_0)^3}\int e^{-i\vec{\Omega}\cdot\vec{x}}\sum_{m=3}^{\infty}\frac{1}{m!}(-\epsilon x^{-1}e^{-x})^m d^3x . \tag{4.13}$$

After carrying out the angular integration, this expression may be written as

$$(2\pi^2\kappa_0{}^3\Omega)\bar{g}_0(\Omega)[L] = \int_0^\infty x\,\sin\Omega x\sum_{m=3}^{\infty}\frac{1}{m!}(-\epsilon x^{-1}e^{-x})^m dx = \frac{1}{2\pi i}\int_0^\infty x\,\sin\Omega x dx\int_{c-i\infty}^{c+i\infty}(p-1)!\,\epsilon^{-p}x^p e^{px}dp$$

$$= -\frac{1}{2\pi i}\int_{c-i\infty}^{c+i\infty}dp\,(p-1)!(p+1)!\,\epsilon^{-p}(\Omega^2+p^2)^{-\frac{1}{2}p-1}\{\sin[(p+2)\tan^{-1}\Omega/p]\} , \tag{4.14}$$

where the contour for the Mellin inversion integral satisfies $-3<c<-2$. Equation (4.14) can be expanded in an ascending series in ϵ by translating the contour to the left. The leading term in this series gives

$$\bar{g}_0(\Omega)[L] = [\epsilon^3/(2\pi^2\kappa_0{}^3)3!][\ln\epsilon + 2\gamma - \tfrac{17}{6} + \tfrac{1}{2}\ln(\Omega^2+9) + 3(\Omega)^{-1}\tan^{-1}(\Omega/3)] . \tag{4.15}$$

This function has branch points at $\Omega=\pm 3i$ and is of order $\epsilon^3\ln\epsilon$. Higher-order terms in the expansion of Eq. (4.14) have branch points still further removed from the real axis of the Ω plane.

We next consider the diagrams of Figs.6(d) and 6(e), whose evaluation is straightforward. Their contributions are listed below:

$$g_0(r)[6d] = \tfrac{1}{2}\epsilon^3x^{-2}[\ln 3(e^{-2x}) + E_1(3x) - e^{-2x}E_1(x)] , \tag{4.16}$$

$$\bar{g}_0(\Omega)[6d] = (\epsilon^3/4\pi^2\kappa_0{}^3\Omega)\{\ln 3\tan^{-1}(\Omega/2) + \int_0^\infty(\sin\Omega x/x)[E_1(3x) - e^{-2x}E_1(x)]dx , \tag{4.17}$$

$$g_0(r)[6e] = -\tfrac{1}{8}\epsilon^3 x^{-2}\{(x+1)e^{-2x}\ln 3 + \tfrac{4}{3}(e^{-3x} - e^{-2x}) + E_1(3x) - e^{-2x}E_1(x) - x[e^{-2x}E_1(x) + E_1(3x)]\}\,, \quad (4.18)$$

$$\bar{g}_0(\Omega)[6e] = (-\epsilon^3/16\pi^2\kappa_0{}^3\Omega)\{\ln 3[\Omega/(\Omega^2+4) + \tan^{-1}(\Omega/2)] + \tfrac{4}{3}[\tan^{-1}(\Omega/3) - \tan^{-1}(\Omega/2)]$$
$$+ \int_0^\infty (\sin\Omega x/x)[E_1(3x) - e^{-2x}E_1(x)]\,dx - [\Omega/(\Omega^2+4)][\tfrac{1}{2}\ln(\Omega^2+9) - (2/\Omega)\tan^{-1}(\Omega/3)]$$
$$- (1/\Omega)[\tfrac{1}{2}\ln(\Omega^2+9) - \ln 3]\}\,. \quad (4.19)$$

Again, both diagrams are $O(e^{-2x})$ as $x \to \infty$, and the Fourier transforms are therefore analytic in the strip $|\mathrm{Im}\Omega| < 2$.

There remains the diagram Fig. 6(f), whose contribution in configuration space is

$$g_0(r)[6f] = \tfrac{1}{2}(-\beta)^5\rho^2 \int d^3r_3 d^3r_4 \phi_s(\vec{r}_3 - \vec{r}_1)\phi_s(\vec{r}_4 - \vec{r}_1)\phi_s(\vec{r}_3 - \vec{r}_4)\phi_s(\vec{r}_2 - \vec{r}_3)\phi_s(\vec{r}_2 - \vec{r}_4)\,. \quad (4.20)$$

In the appendix it is shown that the Fourier transform of this expression can be reduced to the form

$$\bar{g}_0(\Omega)[6f] = \frac{-\epsilon^3}{4\pi^2\kappa_0{}^3}\int_0^1 dx \int_0^1 dy \frac{[1+x(1-x)\Omega^2]^{-1/2}[1+y(1-y)\Omega^2]^{-1/2}}{\Omega^2(x-y)^2 + \{1+[1+x(1-x)\Omega^2]^{1/2} + [1+y(1-y)\Omega^2]^{1/2}\}^2}\,. \quad (4.21)$$

This integral can be expressed in terms of known transcendental functions, but its analytic properties are clear. In the strip $|\mathrm{Im}\Omega| < 2$, since $|x(1-x)| < \frac{1}{4}$ for $0 < x < 1$ the integrand is a continuous function of Ω, x, and y, and is analytic in Ω. Hence $\bar{g}_0(\Omega)[6f]$ is also analytic in $|\mathrm{Im}\Omega| < 2$.

We have shown that up to and including terms of $O(\epsilon^3)$, $\bar{g}_0(\Omega)$ is analytic in the strip $|\mathrm{Im}\Omega| < 2$. The integrand of Eq. (4.4) is therefore analytic in this region except for poles. It has one pole at $\Omega = iB$, where B is real and $B \approx 1$, which can be found by iteration. The dominant term in $g(r) - 1$ will then be given by $2\pi i$ times the residue of the integrand of Eq. (4.4) at the pole $\Omega = iB$. The terms neglected because of the integral along the branch cut are $O(e^{-2x})$. Finally we have

$$g(r) \sim 1 - Ax^{-1}e^{-Bx} + O(e^{-2x})\,, \quad (4.22)$$

where the constants A and B are evaluated below. From Eq. (4.4), B will be given by the solution of the equation

$$-B^2 + 1 + 2\pi^2\kappa_0{}^3\epsilon^{-1}B^2\bar{g}_0(iB) = 0 \quad (4.23)$$

with $\bar{g}_0(\Omega)$ given by the sum of Eqs. (4.6), (4.15), (4.17), (4.19), and (4.21). If we retain only the leading term of $\bar{g}_0(\Omega)$ given by Eq. (4.6) we have

$$B^2 = 1 - (\epsilon/4B)\ln[(2-B)/(2+B)]\,. \quad (4.24)$$

Successive iteration yields

$$B^2 = 1 + \tfrac{1}{4}\epsilon\ln 3 + \tfrac{1}{8}\epsilon^2\ln 3(\tfrac{1}{3} - \tfrac{1}{4}\ln 3) + O(\epsilon^3)\,. \quad (4.25)$$

The remaining diagrams also contribute to $O(\epsilon^2)$ and the complete result is

$$B = 1 + \tfrac{1}{8}\epsilon\ln 3 + (\epsilon^2/12)\ln\epsilon + (\epsilon^2/48)\Big\{8\gamma - \tfrac{34}{3} + 5\ln 3 + \tfrac{27}{8}(\ln 3)^2 + 6\ln 2 + 9\int_0^\infty (\sinh x/x)[E_1(3x) - e^{-2x}E_1(x)]dx$$
$$- 12\int_0^1\int_0^1 dxdy \frac{[1+x(x-1)]^{-1/2}[1+y(y-1)]^{-1/2}}{\{1+[1+x(x-1)]^{1/2}+[1+y(y-1)]^{1/2}\}^2 - (x-y)^2}\Big\} + O(\epsilon^3\ln\epsilon)\,. \quad (4.26)$$

Evaluating the integrals numerically, we have

$$B = 1 + \tfrac{1}{8}\epsilon\ln 3 + (\epsilon^2/12)\ln\epsilon + 0.066\,\epsilon^2\,, \quad (4.27)$$

while from Eq. (4.4), we have

$$A = \epsilon[1 + 8\pi^3\rho B^2 g_0(iB)]/[1 - 8\pi^3\rho g_0(iB) - 4\pi^3\rho iBg_0{}'(iB)] = \epsilon + \tfrac{3}{8}\epsilon^2\ln 3 + \tfrac{1}{6}\epsilon^2 + O(\epsilon^3\ln\epsilon)\,. \quad (4.28)$$

5. CONCLUSION

We remark that if our asymptotic expression for the radial distribution function [Eqs. (4.22), (4.27), and (4.28)] is expanded for distances $x < 8/\epsilon\ln 3$, we recover the asymptotic form of the Bowers-Salpeter result together with higher-order corrections. Our expression gives the radial distribution function over at least the range $1 < x < \infty$, i.e., at all distances beyond the radius of the Debye sphere. At smaller distances, direct expansion of Eq. (4.4) yields the Bowers-Salpeter result identically. Our result implies that the Debye screening distance is not identically

$$\Lambda_D = (4\pi\beta\rho e^2)^{-1/2} , \tag{5.1}$$

but rather $\Lambda_D{}^1$, where

$$\Lambda_D{}^1 = \Lambda_D/[1 + \tfrac{1}{8}\epsilon \ln 3 + (\epsilon^2/12)\ln\epsilon + O(\epsilon^2)] . \tag{5.2}$$

ACKNOWLEDGMENT

The authors are indebted to Dr. Mark Diesendorf both for drawing this problem to their attention and for stimulating discussions. We are grateful to A. J. Guttman for assistance in programming.

APPENDIX

We require the Fourier transform of the integral Eq. (4.20) which is

$$g_0(r)[6f] = \tfrac{1}{2}(-\beta)^5\rho^2 \int\int d^3r_3 d^3r_4\, \phi_S(\vec{r}_3 - \vec{r}_1)\phi_S(\vec{r}_4 - \vec{r}_1)\phi_S(\vec{r}_3 - \vec{r}_4)\phi_S(\vec{r}_2 - \vec{r}_3)\phi_S(\vec{r}_2 - \vec{r}_4) . \tag{A.1}$$

Using the relation [Eq. (2.15) – (2.18)]

$$\phi_S(r) = (e^2/2\pi^2)\int d^3\omega [e^{i\vec{\omega}\cdot\vec{r}}/(\omega^2 + \kappa_0^2)] . \tag{A.2}$$

Equation (A.1) becomes

$$g_0(r)[6f] = \tfrac{1}{2}(-\beta)^5(2\pi)^6\rho^2(e^2/2\pi^2)^5 \int\int\int d^3\omega_1 d^3\omega_2 d^3\omega_3 e^{i(\vec{\omega}_1 + \vec{\omega}_2)\cdot\vec{r}}$$
$$\times \{(\omega_1{}^2 + \kappa_0^2)(\omega_2{}^2 + \kappa_0^2)(\omega_3{}^2 + \kappa_0^2)[(\vec{\omega}_1 + \vec{\omega}_3)^2 + \kappa_0^2][(\vec{\omega}_2 - \vec{\omega}_3)^2 + \kappa_0^2]\}^{-1} . \tag{A.3}$$

The Fourier transform of this expression is then

$$\bar{g}_0(\Omega)[6f] = \tfrac{1}{2}(-\beta)^5(2\pi)^6\rho^2(e^2/2\pi^2)^5$$
$$\times \int\int d^3\omega_1 d^3\omega_3 \{(\omega_1{}^2 + \kappa_0^2)[(\vec{\omega} - \vec{\omega}_1)^2 + \kappa_0^2][\omega_3{}^2 + \kappa_0^2][(\vec{\omega}_1 + \vec{\omega}_3)^2 + \kappa_0^2][(\vec{\omega} - \vec{\omega}_1 - \vec{\omega}_3)^2 + \kappa_0^2]\}^{-1} . \tag{A.4}$$

If we introduce dimensionless variables

$$\vec{\Omega}_1 = \vec{\omega}_1/\kappa_0, \quad \vec{\Omega}_2 = \omega_2/\kappa_0, \quad \vec{\Omega} = \vec{\omega}/\kappa_0 \tag{A.5}$$

and make the transformations

$$\vec{Q} = -\vec{\Omega}_1 - \vec{\Omega}_3, \quad \vec{P} = -\vec{\Omega}_1 , \tag{A.6}$$

Eq. (A.4) becomes

$$\bar{g}_0(\Omega)[6f] = \tfrac{1}{2}(-\beta)^5(2\pi/\kappa_0)^6(\kappa_0 e^2/2\pi^2)^5(1/\kappa_0{}^3)$$
$$\times \int\int d^3P d^3Q \{(P^2+1)[(\vec{P} + \vec{\Omega})^2 + 1][(\vec{Q} - \vec{P})^2 + 1](Q^2+1)[(\vec{Q} + \vec{\Omega})^2 + 1]\}^{-1} . \tag{A.7}$$

The identities

$$\int_0^1 dx/[ax + b(1-x)]^2 = 1/ab \tag{A.8}$$

$$\int d^3q/(q^2 + \alpha^2)[(\vec{q} + \vec{\Omega})^2 + \beta^2]^2 = (2\pi^2/\beta)[\Omega^2 + (\alpha + \beta)^2]^{-1} \tag{A.9}$$

then enable us to write

$$\int d^3Q/(Q^2 + \alpha^2)[(\vec{Q} + \vec{\Omega})^2 + \beta^2][(\vec{Q} + \vec{P})^2 + \gamma^2] = \int_0^1 dx \int d^3Q/[(\vec{Q} + \vec{P})^2 + \gamma^2][(\vec{Q} + x\vec{\Omega})^2 + \delta^2]^2$$
$$= 2\pi^2 \int_0^1 dx/\delta[(P - xQ)^2 + (\gamma + \delta)^2] , \tag{A.10}$$

where $\delta^2 = [x(1-x)\Omega^2 + x\beta^2 + (1-x)\alpha^2]$. (A.11)

Successive application of Eq. (A.10) in Eq. (A.7) yields Eq. (4.21).

[1]A preliminary account of this work was given in D. J. Mitchell and B. W. Ninham, Phys. Letters 27A, 154 (1968).
[2]D. L. Bowers and E. E. Salpeter, Phys. Rev. 119, 1180 (1960).
[3]H. E. DeWitt, Phys. Rev. 140, A466 (1965).
[4]T. J. Lie and Y. H. Ichikawa, Rev. Mod. Phys. 38, 680 (1966).
[5]E. E. Salpeter, Ann. Phys. (N. Y.) 5, 183 (1958).
[6]S. Fujita, A. Isihara, and E. Montroll, Bull. Acad. Roy. Med. Belg. 44, 1018 (1958).
[7]J. E. Mayer and E. W. Montroll, J. Chem. Phys. 9, 2 (1941).
[8]C. W. Hirt, Phys. Fluids 8, 693 (1965).

PHYSICAL REVIEW VOLUME 174, NUMBER 1 5 OCTOBER 1968

Kinetic Equations for Turbulent Plasmas. I. Quasilinear Theory

Setsuo Ichimaru
Department of Physics, University of Illinois, Urbana, Illinois
(Received 12 April 1968)

The Vlasov equation is not applicable for those turbulent plasmas in which certain higher-order correlation functions may play just as important a part as the single-particle distribution function. We construct the many-particle distribution functions by summing certain selected products of the single-particle distribution functions and the pair correlation functions, and show that, in the Rostoker-Rosenbluth fluid limit, those distribution functions satisfy the Bogoliubov-Born-Green-Kirkwood-Yvon (BBGKY) hierarchy and enable us to truncate it at the second equation. The resulting equations contain an asymmetric feature in that the single-particle distribution function develops in time with inclusion of the correlation effects in the collision term, while the time evolution of the pair correlation function is governed by a solution of the linearized Vlasov equation. It is shown explicitly that those kinetic equations become identical to the quasilinear equations without mode coupling if the contribution of the growing plasma oscillation is singled out in the pair correlation function.

I. INTRODUCTION

We consider a system containing N identical particles in a box of volume Ω. Each particle is characterized by the electric charge e and the mass m; we assume a smeared-out background of the opposite charges so that the average space-charge field of the system may be canceled. For an ensemble of similar plasmas, the density in the $6N$-dimensional phase space satisfies the Liouville equation; by taking moments of this equation, and by going to the limit $N\to\infty$ and $\Omega\to\infty$ such that $N/\Omega=n$, the average number density of the particles, one arrives at the Bogoliubov-Born-Green-Kirkwood-Yvon (BBGKY) hierarchy equations for the plasma.[1,2] In order to secure a systematic means to treat the hierarchy equations, it is useful to introduce an expansion scheme with respect to the small plasma parameter, $g=1/n\lambda_D^3$, where λ_D is the Debye length. Truncation of the hierarchy is achieved within this scheme by assuming that the single-particle distribution function may be expanded starting from a term of order g^0; the pair correlation function, from a g^1 term; the ternary correlation function, from a g^2 term; and so on. To the lowest order in g, it then follows that a many-particle distribution function is expressed as a simple product of single-particle distribution functions; with the aid of this ansatz, which is equivalent to the Hartree factorization, one can show that the Vlasov equation is a precise description of the plasma in the limit $g\to 0$.[1,2]

What happens to the above scheme in case there is a reason to suppose that the pair correlation